Cerebral Cortex May 2011;21:1094-1104
doi:10.1093/cercor/bhq181
Advance Access publication September 20, 2010

Reorganization of Inhibitory Synaptic Circuits in Rodent Chronically Injured Epileptogenic Neocortex

Xiaoming Jin[1,2], John R. Huguenard[1] and David A. Prince[1]

[1]Department of Neurology and Neurological Sciences, Stanford University School of Medicine, Stanford, CA 94305, USA and [2]Spinal Cord and Brain Injury Research Group, Department of Anatomy and Cell Biology & Stark Neuroscience Research Institute, Indiana University School of Medicine, Indianapolis, IN 46202, USA

Address correspondence to David A. Prince, Neurology and Neurological Sciences, Stanford University School of Medicine, Room M016, Stanford, CA 94305-5122, USA. Email: daprince@stanford.edu.

Reduced synaptic inhibition is an important factor contributing to posttraumatic epileptogenesis. Axonal sprouting and enhanced excitatory synaptic connectivity onto rodent layer V pyramidal (Pyr) neurons occur in epileptogenic partially isolated (undercut) neocortex. To determine if enhanced excitation also affects inhibitory circuits, we used laser scanning photostimulation of caged glutamate and whole-cell recordings from GAD67-GFP–expressing mouse fast spiking (FS) interneurons and Pyr cells in control and undercut in vitro slices to map excitatory and inhibitory synaptic inputs. Results are 1) the region-normalized excitatory postsynaptic current (EPSC) amplitudes and proportion of uncaging sites from which EPSCs could be evoked (hotspot ratio) "increased" significantly in FS cells of undercut slices; 2) in contrast, these parameters were significantly "decreased" for inhibitory postsynaptic currents (IPSCs) in undercut FS cells; and 3) in rat layer V Pyr neurons, we found significant decreases in IPSCs in undercut versus control Pyr neurons. The decreases were mainly located in layers II and IV, suggesting a reduction in the efficacy of interlaminar synaptic inhibition. Results suggest that there is significant synaptic reorganization in this model of posttraumatic epilepsy, resulting in increased excitatory drive and reduced inhibitory input to FS interneurons that should enhance their inhibitory output and, in part, offset similar alterations in innervation of Pyr cells.

Keywords: caged glutamate, electrophysiology, interneurons, posttraumatic epilepsy, synaptic transmission

Introduction

Reduction in γ-aminobutyric acid (GABA)ergic synaptic inhibition is one of the major mechanisms underlying epileptogenesis after brain injury. Losses of different subtypes of GABAergic interneurons (Dinocourt et al. 2003; Kobayashi and Buckmaster 2003; Magloczky and Freund 2005), decrease in release of GABA from presynaptic terminals or in release probability (Marco and DeFelipe 1997; Li and Prince 2002; Zhang et al. 2009; Zhou et al. 2009; Faria and Prince 2010), changes in type and density of postsynaptic $GABA_A$ receptors (Brooks-Kayal et al. 2001; Ragozzino et al. 2005; Jacob et al. 2008), and increase in intracellular chloride concentration (Nabekura et al. 2002; Jin et al. 2005; Pathak et al. 2007) can all impair the efficacy of synaptic inhibition and contribute to epileptic seizures. How these alterations affect cortical inhibition at the circuit level is not well understood. We previously found axonal sprouting and enhanced excitatory connectivity in layer V pyramidal (Pyr) neurons in partially isolated neocortex, a chronic model of posttraumatic epileptogenesis (Salin et al. 1995; Jin et al. 2006; see Graber and Prince 2006 for review). To obtain a better understanding of cortical inhibitory circuits in epileptogenesis, we need to know if sprouting axons of layer V Pyr neurons also increase their excitatory innervation of inhibitory neurons and whether outputs from interneurons to other interneurons and to Pyr neurons have been altered in the chronically injured cortex. Alterations in the wiring of the inhibitory circuits may result in changes in excitability in the neuronal network that could contribute to epileptogenesis.

In the present experiments, we used laser scanning photostimulation (LSPS) combined with whole-cell patch-clamp recording (Jin et al. 2006) to map and quantify changes in cortical inhibitory circuits in a model of epileptogenic focal cortical injury. There were several reasons for focusing on innervation of fast spiking (FS) interneurons in these experiments: 1) FS interneurons play critical physiological roles in controlling the action potential (AP) output and filtering of excitatory inputs onto Pyr cells within cortical circuits through their GABAergic synapses on somata and proximal dendrites of Pyr cells (DeFelipe 1997; Freund and Katona 2007); 2) these neurons form the largest class of inhibitory cells in the cortex (Uematsu et al. 2008); and 3) alterations in the number, excitability, and synaptic transmission onto inhibitory interneurons and their output onto Pyr cells occur in models of epileptogenesis and human epilepsy (Marco et al. 1996; Jefferys and Traub 1998; Li and Prince 2002; Trotter et al. 2006; Ogiwara et al. 2007; Zhou et al. 2009; Brill and Huguenard 2010; Faria and Prince 2010). We examined excitatory and inhibitory synaptic connections onto parvalbumin/GFP-containing FS interneurons in epileptogenic partial cortical isolations of transgenic mice and also inhibitory connections from interneurons to layer V Pyr neurons. Results show that there is increased excitatory and decreased inhibitory innervation of both FS interneurons and Pyr cells in the injured cortex. The potential functional consequences of these cortical circuit reorganizations after cortical trauma are discussed. Portions of these results have been published in an abstract.

Materials and Methods

Surgical Procedures

All experiments were performed according to protocols approved by the Stanford Institutional Animal Care and Use Committee. Neocortical slices from 41 transgenic mice expressing GFP in cortical FS cells (Chattopadhyaya et al. 2004) at postnatal day P34–P50 (P0: date of birth), and 12 rats aged between P37 and P47 were used for in vitro

recordings. At P21, partially isolated islands of neocortex (undercuts) were produced in 21 mice and 5 rats, using previously described techniques (Hoffman et al. 1994; Li and Prince 2002). Briefly, mice or rats were deeply anesthetized with ketamine (80 mg/kg, intraperitoneally) and xylazine (Rompun 8 mg/kg, intraperitoneally) and mounted in a stereotaxic frame. The scalp was incised, skull exposed, and a bone window opened over the left frontoparietal cortex. A partial isolation of an island of sensorimotor cortex was made using an "L" shaped needle. The needle was inserted tangentially and parasagittally through the dura and lowered to a depth of ~2 mm. It was then rotated 120–135° to produce a contiguous white matter lesion. The skull opening was then covered with sterile plastic wrap (Saran Wrap) and the skin sutured. Animals were allowed to recover for at least 2 weeks (Hoffman et al. 1994; Graber and Prince 1999).

Slice Preparation and Electrophysiology

Animals were deeply anesthetized with pentobarbital (55 mg/kg, intraperitoneally), decapitated, the brain rapidly removed and placed in ice-cold (4 °C) oxygenated slicing solution containing (in mM) 230 sucrose, 2.5 KCl, 1.25 NaH_2PO_4, 10 $MgSO_4.7HO_2$, 10 glucose, 0.5 $CaCl_2.2H_2O$, and 26 $NaHCO_3$. Coronal slices (350 μm) were cut with a vibratome (Lancer Series 1000; Vibratome Company) through the lesioned sensorimotor cortex and from the same region in control animals and maintained using standard techniques (Jin et al. 2006). After ~0.5-h incubation at 32 °C in standard artificial cerbrospinal fluid (ACSF), slices were incubated at room temperature. The ACSF contained (in mM) 126 NaCl, 2.5 KCl, 1.25 NaH_2PO_4, 2 $CaCl_2$, 2 $MgSO_4.7H_2O$, 26 $NaHCO_3$, and 10 glucose; pH 7.4 when saturated with 95% O_2–5% CO_2.

Patch electrodes were pulled from borosilicate glass tubing (1.5 mm outer diameter) and had an impedance of 4–6 MΩ when filled with intracellular voltage-clamp solution containing (in mM): 120 Cs-gluconate, 10 KCl, 11 ethyleneglycol-bis(aminoethylether)-tetraacetic acid (EGTA), 1 $CaCl_2.2H_2O$, 2 $MgCl_2.6H_2O$, 10 *N*-2-hydroxyethylpiperazine-*N*′-2-ethanesulfonic acid (HEPES), 2 Na_2ATP, 0.5 NaGTP, and 0.5% biocytin. In current-clamp experiments, we used a K-gluconate–based intracellular solution containing (in mM): 95 K-gluconate, 40 KCl, 5 EGTA, 0.2 $CaCl_2.2H_2O$, 10 HEPES, and 0.5% biocytin. The osmolarity of the pipette solutions was adjusted to 285–295 mOsm and pH to 7.3 with 1 M KOH. Single slices were transferred to a recording chamber where they were minimally submerged in ACSF. Fifty micrometer 2-amino-5-phosphonovaleric acid (APV) was added to the perfusate to prevent polysynaptic recurrent excitation and eliminate slow N-methyl-D-aspartic acid (NMDA) receptor activation.

Patch-clamp recordings were made from layer V GFP-expressing FS cells in undercut sensorimotor cortex or the same region in control slices, using infrared video microscopy (Zeiss Axioskop; Carl Zeiss) and a ×63 water-immersion lens (Achroplan 63×, 0.9W; Carl Zeiss) and an Axopatch 200A amplifier (Axon Instruments). The responses were low-pass filtered at 2 kHz and saved for later analysis. Excitatory postsynaptic currents (EPSCs) were measured at a holding potential (V_h) of −70 mV, close to the reversal potential for fast GABAergic inhibition, and inhibitory postsynaptic currents (IPSCs) were recorded at V_h = +20 mV, with a calculated reversal potential of −60 mV when the pipettes were filled with the Cs-gluconate internal solution.

Following the electrophysiological recordings, slices containing biocytin-filled neurons were fixed and processed with the standard avidin–biotin–peroxidase method or immunofluorescent staining. Labeled neurons were examined under light and confocal microscopy to verify their morphology and location.

Photolysis of Caged Glutamate and Stimulus Patterns

LSPS by glutamate uncaging was performed as described previously (Jin el al. 2006; Deleuze and Huguenard 2006; Kumar et al. 2007). Briefly, a frequency-tripled Nd:YVO_4 laser (Series 3500 pulsed laser, ~500 mW, 100 kHz repetition rate; DPSS Lasers) was interfaced with an upright microscope (Axioskop, Zeiss) through its epifluorescence port via a series of mirrors and lenses. Movement of the laser beam was controlled with mirror galvanometers (model 6210; Cambridge Technology), which were controlled with scanning and data acquisition software (J.R.H.). Hundred micrometer Montreal Neurological Institute–caged glutamate (4-methoxy-7-nitroindolinyl-caged L-glutamate; Tocris Bioscience) and 50 μM APV (Sigma) were added to 20 mL of recirculating regular ACSF at the beginning of each experiment. Focal photolysis of caged glutamate was accomplished by switching the UV laser to give a 600–1000 μs light stimulus through a ×5 UV objective. To activate neurons in layers II–VI of cortex, spots in a grid of 500–550 × 1000–1200 μm with 50 μm spacing between adjacent spots were flashed in a pseudorandom sequence pattern with a 1-s interval. Each recorded trace consisted of a 100-ms prestimulus baseline and a 500-ms poststimulus period.

Data Acquisition and Analysis

All EPSCs that occurred in time windows between 6–10 ms and 100 ms after photostimulation were regarded as uncaging evoked responses and were included in data analysis. Because direct activation of non-NMDA glutamatergic receptors peaked within 6–10 ms after laser flashes, events occurring during this time window were excluded. While majority of APs evoked by uncaging occurred immediately following laser flashes, about 20% of Pyr neurons fired APs after a >50 ms slow depolarization and one-third of FS cells fired APs repeatedly within ~100 ms following uncaging (data not shown). To optimally detect synaptic connections, all PSCs that occurred within 100 ms after laser flashes were included as evoked responses. EPSCs and IPSCs evoked by uncaging were detected and analyzed using event detection software. To correct for contamination from spontaneous PSCs, we adjusted the cumulative amplitude (defined below) of evoked PSCs for each individual cell by subtracting from each trace the mean PSC amplitude calculated based on prestimulus PSCs.

As in previous studies, we used several parameters to quantify characteristics of synaptic connectivity (Deleuze and Huguenard 2006; Jin et al. 2006). "Hotspots" were sites on the stimulation grid from which at least one evoked postsynaptic current was detected within the measurement window. "Composite amplitude" was defined as the sum of peak amplitudes of all detected synaptic events during the measurement window. "Hotspot ratios," the number of stimulated sites that evoked a PSC divided by the total number of uncaging spots, were computed and plotted with respect to the vertical or horizontal axis by averaging values for each row or column of stimulus sites, respectively. To evaluate the strength and distribution of PSCs, the "region-normalized EPSC or IPSC" was obtained from the sum of all composite amplitudes within a given row or column of stimulus sites along the vertical or horizontal axis divided by the total number of stimulus sites within the column. Statistical significance for group means was determined with a 2-tailed student's *t*-test with a $P < 0.05$. Statistical significances between undercut and control groups and between different vertical or horizontal distances were tested by 2-way analyses of variance (ANOVAs). Further comparisons between control and undercut groups at each individual distance from the soma were made with a student's *t*-test. Data are presented as mean ± standard error of the mean. Origin and Microsoft Excel software were used to perform all statistical analyses.

Results

Cortical GFP-Expressing FS Interneurons

To study excitatory and inhibitory synaptic connectivity to cortical FS interneurons, we used a line of transgenic mice expressing GFP in cortical FS cells (Chattopadhyaya et al. 2004). Coronal brain slices were cut from control and undercut mice, 13–29 days after undercut surgery. To confirm their FS cell identity, we made current-clamp recordings from GFP-expressing cells and filled them with biocytin. All GFP-expressing neurons (17 from the control and 29 from undercut slices), from which AP firing patterns were recorded, exhibited the morphology of multipolar interneurons and fast non-adapting high frequency AP firing (Fig. 1*A*,*B*). All GFP-expressing cells were positive for parvalbumin immunostaining

(data not shown). These experiments confirmed that the GFP-containing cells were FS interneurons.

Excitation Profiles of Cortical FS Neurons and Pyramidal Neurons after Undercut Injury

To compare excitabilities in response to glutamate uncaging between neurons of control and undercut cortex, we used current-clamp recording to map AP firing in layers II–VI Pyr and GFP-expressing FS neurons evoked by LSPS. Grids of photostimulation sites between 350–400 and 350–400 μm with 50 μm spacing were used. Durations of laser flashes were adjusted so that at least one AP could be recorded from each mapping area. In all Pyr neuron maps, laser durations ranged between 600 and 1000 μs, with means of 775 ± 42 μs and 795 ± 53 μs for the control and undercut group, respectively (P > 0.05, student t-test). Mean hotspot number and AP number per map were 2.6 ± 0.3 and 6.1 ± 1.3 for the control group and 2.5 ± 0.3 and 4.0 ± 1.0 for the undercut group (P > 0.05, student t-test, data not shown). LSPS evoked depolarizations and AP firings were mostly evoked by uncaging stimuli located near the recorded somata. Average map sizes of evoked APs were smaller in the undercut group in terms of hotspot and spike number, but these differences did not reach statistic significance; 97.1% and 90.3% of the hotspots were located within 150 μm of somata in the control and undercut group, respectively (Fig. 2*A–C*, n = 20 in control and n = 20 in undercut).

Among all FS neuron maps, laser durations ranged between 300 and 1000 μs, with the means of 607 ± 72 μs and 517 ± 56 μs for the control and undercut group, respectively (P > 0.05, student t-test). Mean hotspot and AP number per map were 3.7 ± 0.5 and 7.3 ± 1.4 for the control group and 3.1 ± 0.6 and 6.9 ± 1.5 for the undercut group (P > 0.05, student t-test, data not shown); 97.1% and 90.3% of the hotspots were located within 150 μm of somata in the control and undercut groups, respectively. There were no significant differences between the 2 groups for hotspot and spike number at different distances from the somata (Fig. 2*D–F*, n = 14 in control and n = 18 in undercut).

These findings indicated that photostimulation of cortical Pyr neurons and FS interneurons evoked similar relatively focused direct activation in control and undercut animals and that the observed differences between control and undercut mice in excitatory and inhibitory synaptic responses described below were attributable to differences in synaptic connectivity rather than differences in somatic responsiveness to photostimulation and uncaged glutamate.

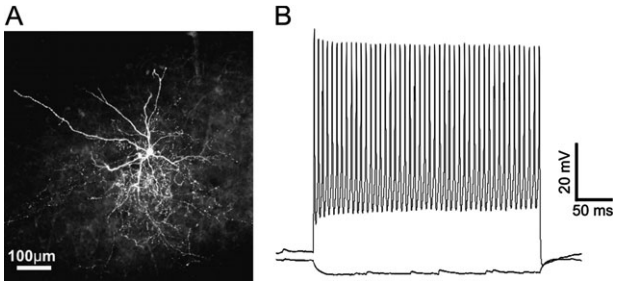

Figure 1. GFP-expressing neurons were FS interneurons. (*A*) A confocal image of a biocytin-filled GFP-expressing neuron in a control 350-μm-thick coronal neocortical slices. This layer V neuron has typical morphology of FS interneurons with smooth multipolar dendrites and a dense local axonal arbor. (*B*) GFP neurons exhibited fast and high frequency AP firing pattern with little adaptation. Scale bar in A: 100 μm.

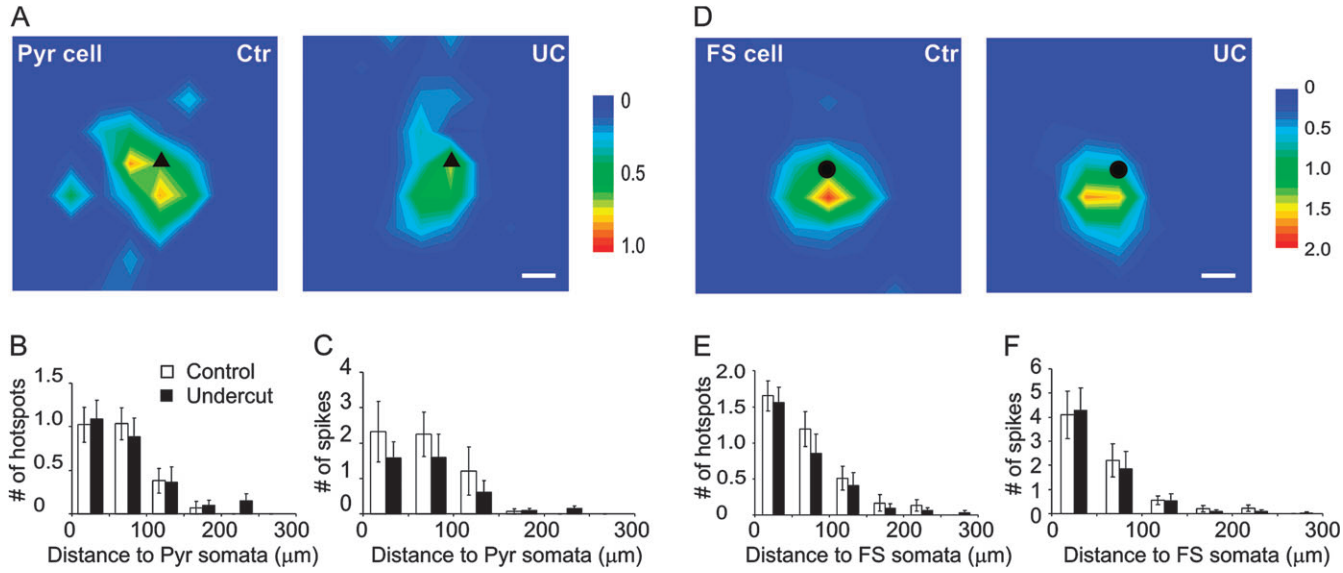

Figure 2. Similar direct excitation profiles of layer V pyramidal (Pyr) neurons and FS interneurons in control and undercut neocortex. (*A*) Average AP maps in Pyr neurons. Areas of 400 × 400 μm were photostimulated by laser flashes with a 50 μm spacing and the mean number of APs evoked by each spot plotted in control (Ctr, left) and undercut neurons (UC, right). Most of the APs were activated by stimuli close to the somata of the recorded neurons. Black triangle: somata of pyr neurons. (*B* and*C*) Analysis of direct excitation profiles in Pyr neurons. There were no significant differences between the control (n = 20) and undercut (n = 20) in average number of hotspots (*B*) and evoked APs (*C*) relative to different distances to somata. (*D*) Average AP maps in FS interneurons. The intensity and size of the average maps were similar between the control and undercut neurons. Black circle: somata of FS cells. (*E* and*F*) Analysis of direct excitation profiles in FS cells. There were no significant differences between the control (n = 14) and undercut (n = 18) in number of hotspots (*E*) and evoked APs (*F*) relative to distances to somata. Note that most APs were generated within a region 150 μm from somata in all average maps. Scale bar in (*A*) and (*D*): 50 μm. Scale to right in (*A*) and (*D*): mean number of APs evoked by spots. White bar: control group; black bar: undercut group.

Increased Excitatory Connectivity to FS Cells in the Undercut Cortex

We previously found significant increases in excitatory connectivity to layer V Pyr neurons in the undercut cortex using the LSPS technique (Jin et al. 2006), results consistent with earlier morphological observations of significant axonal sprouting in these neurons (Salin et al. 1995). This made it important to determine whether the sprouting Pyr neurons also targeted FS interneurons in layer V, a result that would have potential consequences for the functional balance between excitatory and inhibitory activities within the injured cortical network, for example, an increase in excitatory drive onto FS cells could result in a stronger inhibitory output that would in part compensate for the enhanced excitatory connectivity.

To test this hypothesis, we mapped monosynaptic excitatory connectivity onto layer V FS neurons in control and undercut sensorimotor cortex. Whole-cell voltage-clamp recordings were obtained from 19 control and 18 undercut GFP-expressing FS neurons in layer V in the cortex within the "L"-shaped transcortical and undercut lesioned area, visible in the in vitro slices (Graber and Prince 2006), and from a corresponding area of the control cortex. For each recorded neuron, focal photolysis of caged glutamate was used to stimulate a ~0.5 × 1.2 mm region covering cortical layers 2–6 with a grid spacing of 50 μm. We constructed maps of excitatory synaptic input to individual FS neurons and compared input strength across cortical layers based on the composite EPSC amplitude evoked by uncaging at each spot and the fraction of hot spots at which EPSCs could be evoked (Jin et al. 2006). Sample responses from one FS interneuron are shown in Figure 3*A,B*. The above criteria (Materials and Methods) were used to distinguish between direct activation (Fig. 3*B*-3) and synaptic responses (Figs 3*B*-2 and 4). Average maps from 19 control and 18 undercut FS cells are shown in Figure 3*C,D*.

We analyzed the changes in region-normalized EPSC amplitude and hotspot ratio relative to the cortical depth of

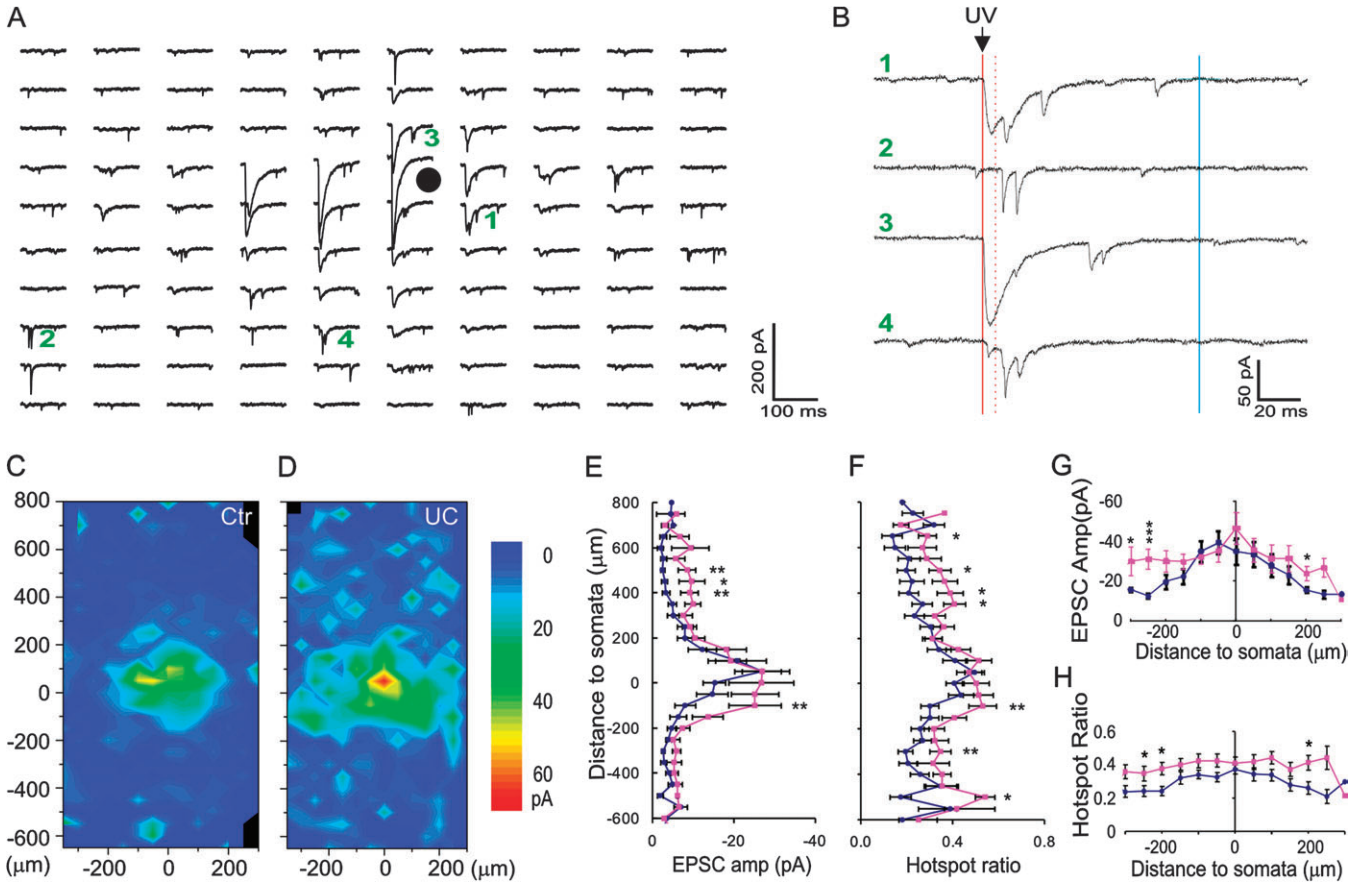

Figure 3. Enhancement of excitatory synaptic input onto layer V FS interneurons in the undercut cortex. (*A* and *B*) Recording traces in a central field of a representative map. Each trace in (*A*) corresponds to an uncaging spot, with 50 μm spacing. Black circle in (*A*): FS cell soma. Traces labeled with green numbers are expanded and shown on the right in (*B*). The red solid line indicates the time of UV laser flash, between solid and dotted red line is the time of direction activation (6–8 ms), synaptic events during dotted red line and blue line (100 ms) were detected as evoked responses. At some uncaging sites, both direct activation and EPSCs were triggered but with different latencies (e.g., 1, 3, and 4), whereas only EPSCs were evoked at other locations (e.g., 2). (*C* and *D*) Average maps of the composite amplitude of EPSCs in layer V FS cells of the control (C, $n = 19$) and undercut (*D*, $n = 18$) groups. Most neurons received major excitatory inputs from layer V and less from other layers. Scale bar: composite amplitude of trigged events (pA, same for all following maps). (*E–H*) Differences in region-normalized EPSC amplitude (*E* and *G*) and mean hotspot ratio (*F* and *H*) at various vertical and horizontal distances from somata in the control and undercut groups. Two-way ANOVAs indicated highly significant differences in all comparisons between the 2 groups ($P < 0.0001$ for all). (*E* and *F*) Data were plotted along cortical depths. Increases in both parameters were most obvious in areas close to layer V and layer II/III. 0: position of somata; positive along *y*-axis: toward pial surface; negative along *y*-axis: toward white matter. (*G* and *H*) Data were plotted along horizontal direction. Significant increases were present at several horizontal distances from the somata. The differences were not related to the position of the laser spots in relation to the transcortical cut ($P > 0.05$, 2-way ANOVA). *x*-axis positive and negative: lateral and medial to somata, respectively. $^{*}P < 0.05$; $^{**}P < 0.01$; $^{***}P < 0.005$ in this and subsequent figures (post hoc student's *t*-test).

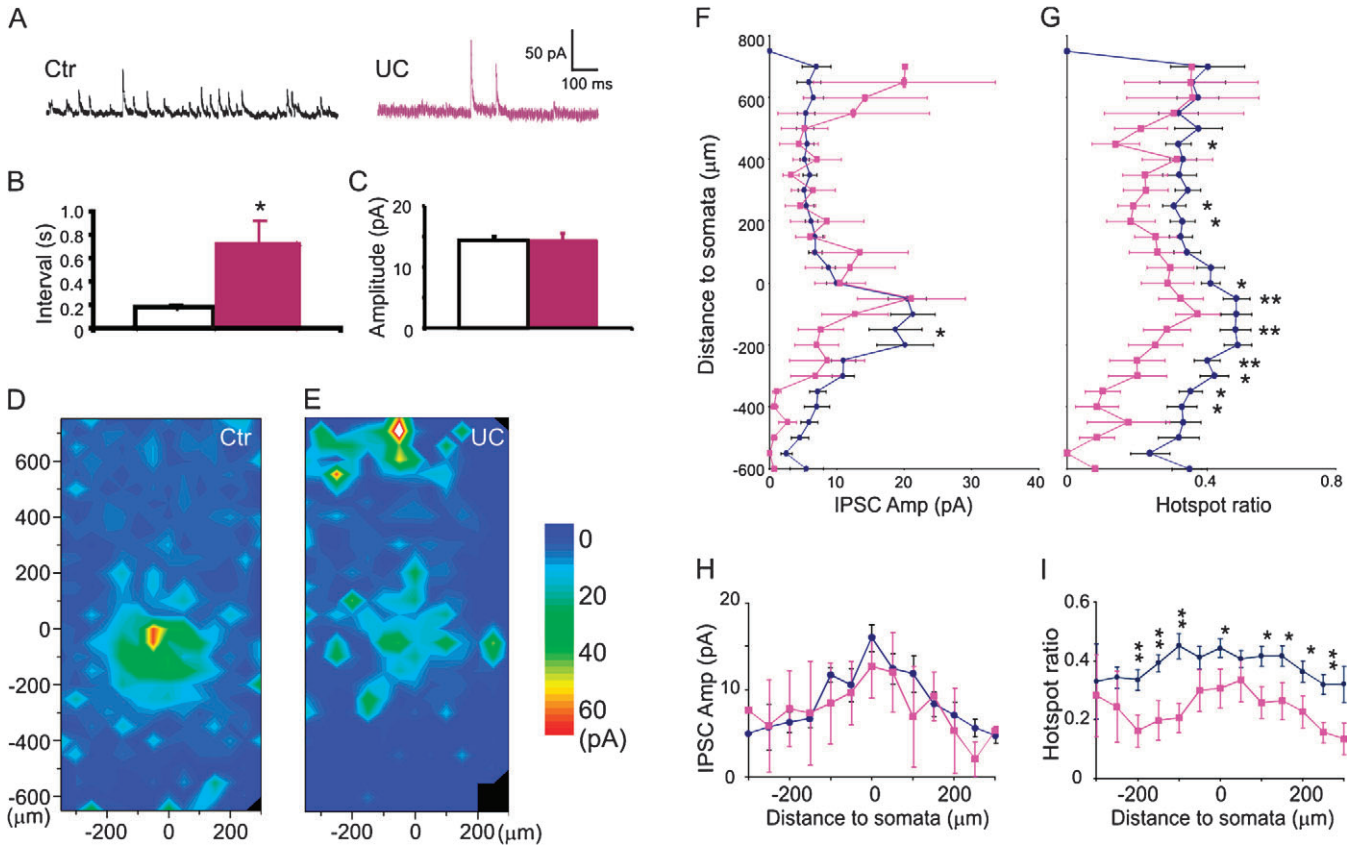

Figure 4. Reduced inhibitory synaptic connectivity onto layer V FS interneurons in the undercut cortex. (*A*) Sample traces of spontaneous IPSCs recorded from control and undercut FS cells with $V_h = +20$ mV. (*B*) Interevent intervals of sIPSCs were much longer in undercut (red bar) than in the control (white bar; 0.17 ± 0.03 s in control and 0.71 ± 0.21 s in undercut, $P < 0.005$, Student's *t*-test). (*C*) There was no difference in mean sIPSC amplitude. (*D* and *E*) Average maps of the composite amplitude of IPSCs in layer V FS cells of the control (*D*, $n = 24$) and undercut (*E*, $n = 14$) groups. Evoked events were detected in time windows between 0 and 100 ms of uncaging stimulus onset. (*F–I*) Differences in region-normalized IPSC amplitudes (*F* and *H*) and mean hotspot ratio (*G* and *I*) at various vertical and horizontal distances from somata in the control and undercut groups. Two-way ANOVAs indicated significant to highly significant differences in all comparisons between the 2 groups. (*F* and *G*) Data were plotted along cortical depths. Increases in hotspot ratio exist across all cortical layers except layer II/III, where hotspot ratio remained unchanged, while region-normalized amplitude became larger. (*H* and *I*) Region-normalized IPSC amplitude (*H*) and hotspot ratio (*I*) plotted along horizontal direction. Significant increases in hotspot ratio were present along horizontal distances from the somata.

the uncaging stimulus. In the normal sensorimotor cortex, most excitatory input onto layer V FS neurons was from a region within 150–200 μm of the soma, within the extent of layer V; inputs from other laminae contributed significant less (Fig. 3*C*). In addition to highly significant differences in region-normalized EPSC amplitude and mean hotspot ratio at different cortical depths within control slices (Fig. 3*E,F*) ($F = 6.8$, $P < 0.0001$ and $F = 4.9$, $P < 0.0001$, respectively, 2-way ANOVA), there were highly significant differences between the control and undercut group in region-normalized EPSC amplitude and hotspots ratio ($F = 21.4$, $P < 0.0001$ and $F = 43.6$, $P < 0.0001$, respectively, 2-way ANOVA). The increases in region-normalized EPSC amplitude and hotspot ratio included most layers of the cortex (Fig. 3*C–F*; $P < 0.05$ to $P < 0.005$, student *t*-test). Specifically, there were significant increases in region-normalized EPSC amplitude and hotspot ratio in areas 100, 300, and 500 μm below the somata ($P < 0.05$ to $P < 0.005$, student *t*-test) and 350–500 μm superficial to the somata in layer V ($P < 0.05$ to0.01, student *t*-test). The mean increases in region-normalized EPSC amplitude and hotspot ratio across all layers were 1.9- and 1.5-fold, respectively, but the increases were 3.0- and 1.7-fold, respectively, for areas 350–700 μm superficial to the somata. These data suggest that layer V FS neurons in the undercut cortex receive more widespread excitatory synaptic input, most prominently from excitatory cells in layer II/III and layer V.

We also plotted these data along a horizontal (intercolumnar) direction with respect to the recorded somata to compare the extent of the increase in the excitatory synaptic connectivity from areas medial and lateral to the recorded cells. Two-way ANOVAs indicated that region-normalized EPSC amplitude and hotspot ratio along horizontal distance were significantly different ($F = 3.0$, $P < 0.001$ and $F = 2.3$, $P < 0.01$, respectively), with neurons in the undercut cortex having a significantly larger region-normalized EPSC amplitude and a greater hotspot ratio ($F = 18.3$, $P < 0.0001$ and $F = 41.3$, $P < 0.0001$, respectively, 2-way ANOVA) at distances of 100 and 200 μm medial and 250 μm lateral to the somata ($P < 0.05$, Fig. 3*G*), as well as greater hotspot ratio at distances of 50–150 μm and 250 μm medial and 50–150 μm, and 250 μm lateral to the somata ($P < 0.05$ to $P < 0.01$, Fig. 3*H*).

To further assess excitatory synaptic inputs onto FS cells, we recorded spontaneous EPSCs (sEPSCs) at the beginning of each mapping experiment. EPSCs in FS cells were fast and very frequent, with mean 10–90% rise times of 0.86 ± 0.05 ms and 0.78 ± 0.05 ms and decay time constants of 1.33 ± 0.21 ms

and 1.40 ± 0.15 ms for the control and undercut groups, respectively. The mean interevent intervals were 0.039 ± 0.006 s and 0.043 ± 0.007 s, and the mean amplitudes −13.9 ± 0.6 pA and −14.7 ± 1.2 pA for control and undercut groups, respectively (n = 17 for the control and n = 11 for the undercut group, data not shown). We did not find significant differences between the 2 groups in rise time, decay time, interevent interval, or amplitude of sEPSCs in FS cells ($P > 0.05$, student t-test).

Reduced Inhibitory Connectivity to Layer V FS Interneurons

Cortical FS cells tend to be chemically coupled to each other to form synchronous networks; they less frequently receive inhibitory synaptic input from other subclasses of interneurons such as low threshold spiking cells (Gibson et al 1999; Markram et al. 2004). To determine whether the inhibitory innervation of cortical FS cells is altered after epileptogenic traumatic brain injury, we recorded sIPSCs and also mapped the inhibitory connectivity using LSPS. By shifting V_h to +20 mV, the amplitude of IPSCs was optimized and EPSCs minimized.

We recorded spontaneous IPSC events at the beginning of each mapping experiment. The mean interevents intervals were 0.17 ± 0.03 s (n = 23) and 0.71 ± 0.21s (n = 15) for control and undercut group, respectively (Fig. 4*A–B*, $P < 0.005$, student t-test), indicating that the inhibitory drive onto FS cells in the undercut cortex was markedly reduced. However, the mean amplitudes of sIPSCs were similar between the 2 groups (Fig. 5*A,C* 14.4 ± 0.6 pA and 14.5 ± 1.1 pA for control and undercut group, respectively, $P > 0.05$, student t-test).

Uncaging stimuli evoked IPSCs as outward currents with a large variability in amplitude and latencies of ~3 to 10 ms from the laser flash. In IPSC maps of control animals, most events were evoked in a circular area of ~150 μm around somata in layer V (Fig. 4*D*). In the undercut mice, there were significant reductions in region-normalized IPSCs and hotspot ratio compared with control maps (Fig. 4*D–G*). There were highly significant laminar differences in region-normalized IPSC amplitude and hotspot ratio (F = 5.3, $P < 0.0001$ and F = 2.6, $P < 0.0001$, 2-way ANOVA) and between the control and undercut group in region-normalized IPSC amplitude and hotspot ratio (F = 7.4, $P < 0.01$ and F = 97.8, $P < 0.0001$, respectively, 2-way ANOVA). Along the vertical depth of the

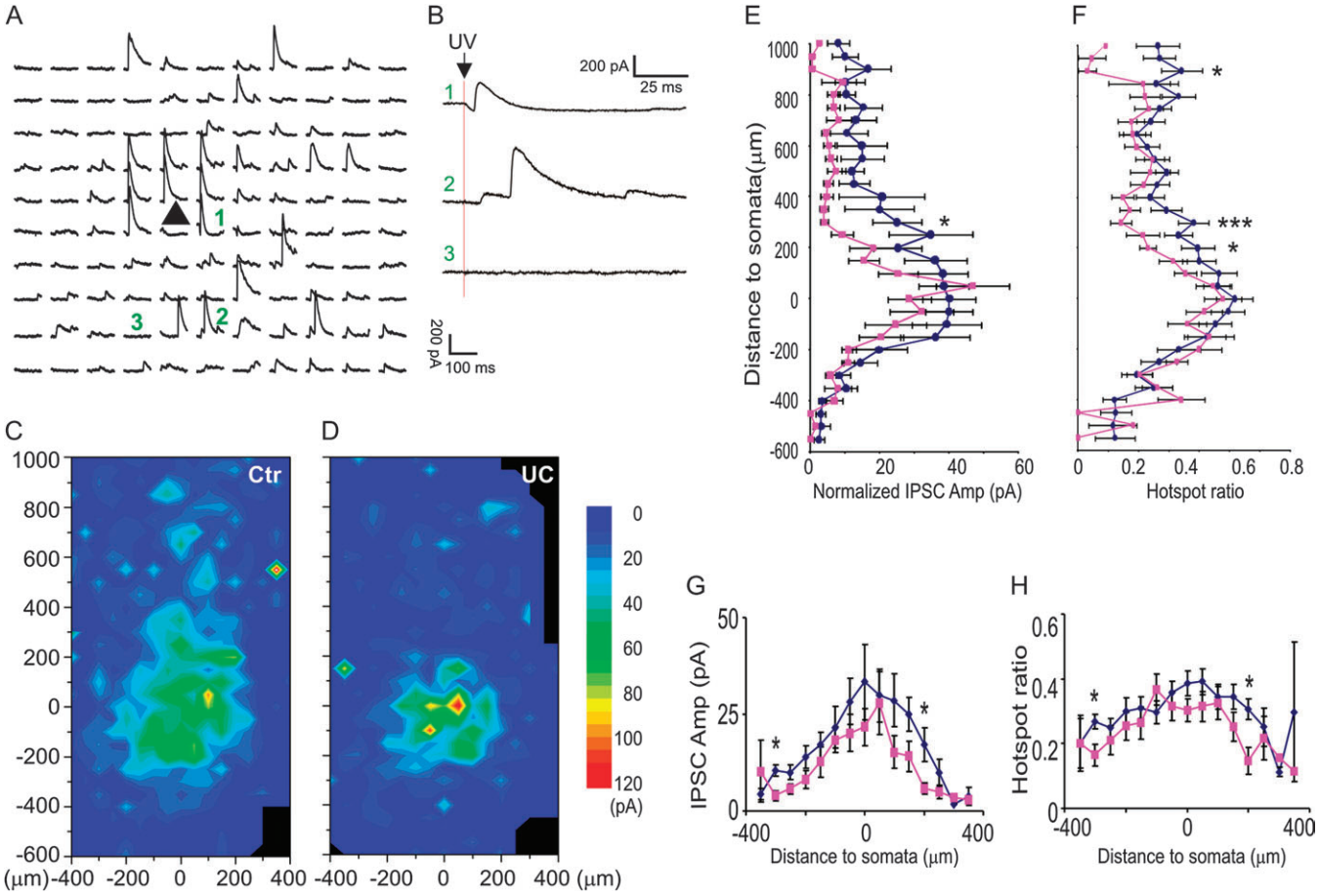

Figure 5. Reduced inhibitory synaptic connectivity onto layer V Pyr neurons in the undercut cortex. (*A* and *B*) Recording traces in a central field of a representative map with 50 μm spacing. Traces labeled with green number are expanded and shown on the right in (*B*). At some uncaging sites, both direct activation and IPSCs were triggered (e.g., trace 1), whereas only IPSCs were evoked at other locations (e.g., trace 2). (*C* and *D*) Average maps illustrate the composite amplitude of detected IPSCs with onset within 100 ms of photostimulation in control (n = 21) and undercut cortex (D, n = 21). In the undercut cortex, the average area making inhibitory synaptic connection onto layer V Pyr neurons was smaller than that in the control. (*E* and *F*) Plots of region-normalized IPSC amplitudes (*E*) and hotspot ratio (*F*) versus vertical distance from the somata. There were significant decreases in region-normalized IPSC amplitude and hotspot ratio ($P < 0.001$ in both parameters, 2-way ANOVA). (*G* and *H*) Plot of mean composite EPSC amplitude (*G*) and hotspot ratio (*H*) evoked by uncaging stimuli in layer V showing significant decreases at several horizontal distances from the somata. x-axis positive and negative: lateral and medial to somata, respectively ($P < 0.05$, 2-way ANOVA).

cortex, there were significant reductions in hotspot ratio that extended from 400 μm above to 600 μm deep to the somata (Fig. 4*G*; $P < 0.05$ to $P < 0.01$, *t*-test), while reductions in region-normalized IPSCs were much smaller in magnitude (Fig. 4*F*), suggesting that shrinkage of inhibitory synaptic maps was mainly caused by a reduction in the connectivity of functionally coupled presynaptic interneurons.

Interestingly, there was a significant increase in region-normalized IPSC amplitude in a superficial cortical area, in a 50 μm band corresponding to layer II (Fig. 4*E*,*F*; $P < 0.05$, student *t*-test). This increase was mainly due to an increase in the region-normalized amplitude ((Fig. 4*F*, $P < 0.05$, *t*-test), suggesting an increase in the strength of inhibitory synaptic coupling from layer II to layer V FS cells. However, this finding is of uncertain significance due to the low incidence in our sample (only in 2 of 12 layer V FS cells) and the fact that there was no similar increase in inhibitory connections from layer II/III to layer V pyramidal neurons (Fig. 5*D*).

Plots of these data along the horizontal axis showed homogenous decreases in hotspot ratio up to 250 μm lateral or medial to the somata (Fig. 4*I*, $P < 0.001$, 2-way ANOVA), while decrease in region-normalized amplitude in the undercut group was not statistically significant (Fig. 4*H*, $P > 0.05$, 2-way ANOVA).

Reduced Inhibitory Connectivity to Layer V Pyramidal Neurons in Rats

The frequency of spontaneous and miniature GABAergic IPSCs is significantly decreased in rat layer V Pyr neurons of the partial cortical isolation (Li and Prince 2002) and inhibition is also reduced in neurons in other models of epileptogenesis (Ribak et al. 1979; Sloviter 1987; Franck et al. 1988; Zhu and Roper 2000; Cossart et al. 2005). To find out if there is a reduction in inhibitory synaptic connectivity in the undercut model, we mapped IPSCs onto rat layer V Pyr neurons, using an approach similar to that for IPSCs in FS cells, and a V_h of 0–10 mV, near E_{EPSC}.

In control slices, uncaging stimuli in layers II–VI evoked inhibitory synaptic input to the Pyr neurons, however, the majority of IPSCs were evoked from layers V and IV, within a range of ~250 μm below and ~400 μm above the somata (Fig. 5*A*,C; see also Salin and Prince 1996). The distribution of inhibitory synaptic input was similar in neurons of the undercut and the control in that IPSC amplitude and hotspot ratio increased as the uncaging stimulus approached the soma (Fig. 5*A*,C–F). Along the vertical axis through the cortex, there were significant decreases at several levels in region-normalized IPSC amplitude and hotspot ratio in the population of undercut neurons versus control cells ($F = 22.3$, $P < 0.001$ and $F = 18.0$, $P < 0.001$, respectively, 2-way ANOVA, Fig. 5*D*–*F*). In the undercut group, there were significant decreases in hotspot ratio in areas 200, 300 and 900 μm above somata ($P < 0.05$ to $P < 0.01$, student *t*-test) and decrease in region-normalized EPSC amplitude in an area 300 μm above somata ($P < 0.05$, student *t*-test). Results suggested that inhibitory connectivity onto layer V Pyr cells was significantly reduced in the undercut cortex. When these data were plotted along the horizontal axis, the hotspot ratio and region-normalized amplitude in the undercut group were significantly smaller than the control group (Fig. 5*H*, $P < 0.01$ in both between the 2 groups, 2-way ANOVA).

Discussion

We used LSPS in combination with whole-cell patch-clamp recordings to study synaptic reorganization in inhibitory neuronal circuits in the undercut model of posttraumatic epileptogenesis in rats and mice. We found a significant increase in excitatory and decrease in inhibitory synaptic connectivity onto layer V FS interneurons in mice, together with significant decreases in inhibitory synaptic connectivity onto layer V Pyr neurons in epileptogenic rat neocortex. These changes had a distribution through the cortex that was generally more marked in perisomatic areas. Together with previous results showing increased excitatory synaptic connections onto layer V Pyr neurons in the same model (Jin et al. 2006), the current data suggest that connections of Pyr cells and FS interneurons are similarly affected by the injury, that is, both cell types show increases in excitatory and decreases in inhibitory synaptic inputs. Neither the increased excitatory innervation, presumably due to new connections made by sprouting Pyr cell axons, nor the decreased inhibitory connectivity from FS and other interneurons appear to be target selective. The net functional effect of this reorganization in cortical inhibitory and excitatory circuits is known to be emergence of epileptogenesis, which likely indicates that effects on pyramidal neurons predominate.

Enhanced Excitatory Connectivity to FS Cells

Layer V FS interneurons receive EPSCs with faster kinetics and higher frequency than pyramidal neurons (Thomson 1997; Povysheva et al. 2006). These events originate largely within the same layer (Fig. 3*C*). In contrast, an earlier LSPS study showed that FS cells in layer II/III receive strongest excitatory input from layers IV and Va and moderately strong activation from layer II/III (Dantzker and Callaway 2000). Paired recording data suggest that layer V interneurons receive the majority of their excitatory synaptic input from layer V and less from layer II/III (Thomson and Bannister 2003). Morphologically, layer V FS cells form dense spherical local axonal arbors, suggesting that they provide inhibitory control for nearby excitatory and inhibitory neurons (Fig. 1*A*; Kawaguchi and Kubota 1997). Taken together, these findings indicate that layer V FS cells function mainly in regulating intralaminar network excitability.

In EPSC maps, we found increases in both region-normalized amplitude and hotspot ratio in layer V FS interneurons of the undercut cortex. The increases were larger for hotspot ratio than for region-normalized amplitudes, suggesting that presynaptic excitatory neurons are coupled to a greater number of postsynaptic FS cells but do not increase the numbers of contacts onto individual targets. We previously reported a similar expansion of EPSC maps in layer V pyramidal neurons of epileptogenic cortex in this model (Jin et al. 2006). In the hippocampus, many studies suggest that sprouting mossy fiber axons predominantly form recurrent excitatory circuits by forming synapses in the granular and molecular layers (Buckmaster et al. 2002; Sutula 2002; Scharfman et al. 2003; Sutula and Dudek 2007), however, there is also evidence that sprouting mossy fibers make new synapses onto interneurons, particularly parvalbumin-containing neurons in the granule cell layer (Kotti et al. 1997; Sloviter et al. 2006). Our data in epileptogenic neocortex also indicate that sprouting axons of the excitatory neurons synapse onto both other excitatory

(Pyr) cells and inhibitory (FS) interneurons. The axons of normal Pyr cells consistently take a relatively straight course through neuropil and show no specificity in terms of axonal trajectories but have a higher potential for contributing to remodeling of synaptic circuit connectivity (Stepanyants et al. 2004). One possible consequence of an increase in excitatory connectivity onto layer V FS cells is to enhance cortical inhibition, which may potentially counteract the enhanced excitation so that the neuronal circuits maintain a balance between excitation and inhibition. The emergence of epileptiform activity in the partially isolated cortex might suggest that the increased excitatory and decreased inhibitory inputs onto FS interneurons are insufficient to counteract the new recurrent excitation of Pyr cells. However, numerous other consequences of the injury are present that may influence network excitability and the outcome, such as alterations in Cl^- transport (Nabekura et al. 2002; Jin et al. 2005), changes in expression of Na^+/K^+ ATPase (Clapcote et al. 2009; Chu et al. 2009), the release of cytokines (Jankowsky and Patterson 2001), etc. Also, maneuvers that enhance synaptic excitation and inhibition in parallel may still result in hyperexcitability and epileptiform discharge in cortical networks, perhaps due to the much higher density of excitatory connections (e.g., Rutecki et al. 1987).

In the normal neocortex, excitatory neurons and interneurons make precise layer-specific synaptic connections (Somogyi et al. 1998; Larsen and Callaway 2006). This pattern of precise connectivity is altered within 2–3 weeks after injury in that sprouting excitatory axons make more diffuse connections to pyramidal neurons and interneurons (Fig. 3*D*; Salin et al. 1995). Whether the enlarged connectivity map can be further refined by processes such as axonal pruning and synapse elimination (e.g., Stevens et al. 2007) requires further investigation. It is possible that the regenerative response is a dynamic process that evolves over a long period of time, involving axonal sprouting, synaptic formation, and elimination (Marchenko et al. 2004; Deller et al. 2006).

Reduced Inhibitory Connectivity to FS Cells

As is the case with EPSC maps, inhibitory synaptic connectivity to layer V FS neurons in control cortex mainly originates from layer V. Cortical FS neurons are often interconnected to other FS cells of the same cortical laminae through chemical and electrical synapses and are less commonly coupled to other subtypes of interneurons such as low-threshold spiking cells (Gibson et al. 1999; Galarreta and Hestrin 2002; Markram et al. 2004). The inhibitory synaptic output from these neurons usually targets somata and proximal dendrites, resulting in large amplitude IPSCs (Somogyi et al. 1998; Xiang et al. 2002). Based on these considerations, we speculate that layer V FS cells make a major contribution to the inhibitory input maps recorded from GFP-expressing layer V FS interneurons.

In the undercut cortex, reduction in IPSC maps of layer V FS cells were mainly due to a decrease in hotspot ratio across different cortical layers, that is, fewer sites from which uncaging evoked IPSCs, suggesting that fewer presynaptic interneurons are efficiently connected to the FS cells. This may result from a reduction in one or more factors including the number of interneurons, the total length of their axonal arbors, the number of GABAergic synapses, or release probability at synapses. No significant decrease in the number of FS cells has been detected in this model of posttraumatic epileptogenesis (Graber K, Prince DA, unpublished data). However, an analysis of biocytin-filled FS cells has revealed several anatomical abnormalities, including large reductions in the length of axonal arbors and a shift toward smaller axonal boutons that contain less immunoreactivity (IR) for vesicular GABA transporter (VGAT1) and are less likely to be closely opposed to postsynaptic gepherin-IR (Shen et al. 2005; Prince et al. 2009). Recent experiments have shown that there is a decreased release probability from interneurons onto layer V Pyr cells in the undercut model (Faria and Prince 2010), results that might be a consequence of these anatomical alterations. Furthermore, an electron microscope analysis has shown that there is a decreased density of symmetrical synapses on somata of layer V Pyr cells of undercut cortex (Wenzel J, Schwartzkroin PA, Prince DA, unpublished data). These morphological data are compatible with a decrease in the number of functional axonal boutons in FS cells and can at least partially explain the reduction in hotspot ratio in the inhibitory maps reported here.

Reduced Inhibitory Connectivity to Pyramidal Neurons in Layer V

Cortical layer V pyramidal neurons normally receive inhibitory synaptic input from interneurons of all cortical layers, with the strongest being from layers V and IV and relatively less from layer II/III (Fig. 5*C*). This result is generally consistent with earlier studies using electrophysiological and LSPS mapping techniques (Salin and Prince 1996; Schubert et al. 2001, 2006).

In this model of posttraumatic epileptogenesis, the increase in excitatory and decrease in inhibitory synaptic connectivity onto FS cells should increase their AP output and, in turn, generate stronger inhibitory drive onto layer V pyramidal cells. However, our data suggest that this is not the case. We found that there were decreases in hotspot ratio and region-normalized IPSC amplitude in layer V Pyr cells of undercut cortex when uncaging stimuli were applied mainly in areas 200–250 μm and 950 μm superficial to the somata, which would correspond approximately to layer IV and layer II, respectively. Several factors may contribute to this apparent discrepancy. First, the reduction in inhibitory input map for layer V Pyr neurons is different from that for FS cells. In FS cells, significant reductions in hotspot ratio occur across most cortical layers, particularly layers V and VI (Fig. 4*E,G*). In contrast, in Pyr neurons, the reductions in inhibitory input map occur mainly in layers IV and II, with almost no change in layer V (Fig. 5*D,F*), suggesting a loss of interlamina but preservation of intralaminar inhibition to the layer V Pyr neurons. Second, different types of interneurons may react differently to traumatic brain injury (Cossart et al. 2005) so that alterations in synaptic connectivity from different types of interneuron vary considerably. In hippocampus, somatostatin-containing interneurons are the most vulnerable in different models of temporal lobe epilepsy (Buckmaster and Jongen-Relo 1999; Dinocourt et al. 2003) and loss of somatostatin-containing and parvalbumin-containing neurons contributes to alterations in dendritic and somatic inhibition, respectively (Dinocourt et al. 2003; Cossart et al. 2005). In the neocortex, preferential loss of inhibitory neurons has been documented in chronic undercuts in cats (Avramescu et al. 2009). Alterations in several subtypes of GABAergic interneurons occur in other epileptogenic lesions (Rosen et al. 1998; Spreafico et al. 1998; DeFelipe

1999; Kharazia et al. 2003). Somatostatin and parvalbumin immunoreactive interneurons exhibit high vulnerability to glutamate excitotoxicity (Weiss et al. 1990; Buriticá et al. 2009). In addition, in the neonatal freeze lesion model, short latency inhibition from presumed basket cells is actually enhanced compared with controls (Brill and Huguenard 2010). The combination of differences in vulnerability after injury and in axonal targeting from subtypes of interneurons to pyramidal neurons (Kawaguchi and Kubota 1997) will likely contribute to the high variability in the inhibitory output to layer V pyramidal neurons. Third, because FS interneurons make a significant contribution to synaptic inhibition in Pyr neurons (DeFelipe 1997; Freund and Katona 2007), the decrease in IPSC maps is probably due to a decrease in the number of functional axonal boutons of FS cells, as discussed above. Finally, recent results indicate that a decreased probability of GABA release from inhibitory terminals onto both Pyr cells and FS interneurons is present in the partial cortical isolation model and might contribute, along with changes in circuitry, to results of laser mapping experiments (Ma and Prince 2009; Faria and Prince 2010).

Conclusions

Using the LSPS technique and whole-cell recordings, we found that layer V Pyr neurons in the undercut cortex made enhanced recurrent excitatory connectivity among themselves and onto FS interneurons, while inhibitory connectivity to FS cells and Pyr neurons was decreased. The net increase in excitation and decrease in inhibition onto Pyr neurons may contribute to the generation of epileptic seizures following traumatic brain injury.

Funding

National Institute of Neurological Disorders and Stroke at the National Institutes of Health (5K99NS57940-2, NS12151, NS39579 and DA15043).

Notes

Conflict of Interest: None declared.

References

Avramescu S, Nita DA, Timofeev I. 2009. Neocortical post-traumatic epileptogenesis is associated with loss of GABAergic neurons. J Neurotrauma. 26(5):799–812.

Brill J, Huguenard JR. 2010. Enhanced infra- and supragranular synaptic input onto layer 5 pyramidal neurons in a rat model of cortical dysplasia. Cerb Cortex. 20(5):1093–1105.

Brooks-Kayal AR, Shumate MD, Jin H, Rikhter TY, Kelly ME, Coulter DA. 2001. gamma-Aminobutyric acid(A) receptor subunit expression predicts functional changes in hippocampal dentate granule cells during postnatal development. J Neurochem. 77:1266–1278.

Buckmaster PS, Jongen-Rêlo AL. 1999. Highly specific neuron loss preserves lateral inhibitory circuits in the dentate gyrus of kainate-induced epileptic rats. J Neurosci. 19(21):9519–9529.

Buckmaster PS, Zhang GF, Yamawaki R. 2002. Axon sprouting in a model of temporal lobe epilepsy creates a predominantly excitatory feedback circuit. J Neurosci. 22:6650–6658.

Buriticá E, Villamil L, Guzmán F, Escobar MI, García-Cairasco N, Pimienta HJ. 2009. Changes in calcium-binding protein expression in human cortical contusion tissue. J Neurotrauma. 26(12):2145–2155.

Chattopadhyaya B, Di Cristo G, Higashiyama H, Knott GW, Kuhlman SJ, Welker E, Huang ZJ. 2004. Experience and activity-dependent maturation of perisomatic GABAergic innervation in primary visual cortex during a postnatal critical period. J Neurosci. 24:9598–9611.

Chu Y, Parada I, Prince DA. 2009. Temporal and topographic alterations in expression of the alpha3 isoform of Na+, K(+)-ATPase in the rat freeze lesion model of microgyria and epileptogenesis. Neuroscience. 162(2):339–348.

Clapcote SJ, Duffy S, Xie G, Kirshenbaum G, Bechard AR, Rodacker Schack V, Petersen J, Sinai L, Saab BJ, et al. 2009. Mutation I810N in the alpha3 isoform of Na+, K+-ATPase causes impairments in the sodium pump and hyperexcitability in the CNS. Proc Natl Acad Sci U S A. 106(33):14085–14090.

Cossart R, Bernard C, Ben-Ari Y. 2005. Multiple facets of GABAergic neurons and synapses: multiple fates of GABA signaling in epilepsies. Trends Neurosci. 28(2):108–115.

Dantzker JL, Callaway EM. 2000. Laminar sources of synaptic input to cortical inhibitory interneurons and pyramidal neurons. Nat Neurosci. 7:701–707.

DeFelipe J. 1997. Types of neurons, synaptic connections and chemical characteristics of cells immunoreactive for calbindin-D28K, parvalbumin and calretinin in the neocortex. J Chem Neuroanat. 14:1–19.

DeFelipe J. 1999. Chandelier cells and epilepsy. Brain. 122:1807–1822.

Deleuze C, Huguenard JR. 2006. Distinct electrical and chemical connectivity maps in the thalamic reticular nucleus: potential roles in synchronization and sensation. J Neurosci. 16;26(33):8633–8645.

Deller T, Haas CA, Freiman TM, Phinney A, Jucker M, Frotscher M. 2006. Lesion-induced axonal sprouting in the central nervous system. Adv Exp Med Biol. 557:101–121.

Dinocourt C, Petanjek Z, Freund TF, Ben Ari Y, Esclapez M. 2003. Loss of interneurons innervating pyramidal cell dendrites and axon initial segments in the CA1 region of the hippocampus following pilocarpine-induced seizures. J Comp Neurol. 459:407–425.

Faria LC, Prince DA. 2010. Presynaptic inhibitory terminals are functionally abnormal in a rat model of posttraumatic epilepsy. J Neurophysiol. 104(1):280–290.

Franck JE, Kunkel DD, Baskin DG, Schwartzkroin PA. 1988. Inhibition in kainate-lesioned hyperexcitable hippocampi: physiologic, utoradiographic, and immunocytochemical observations. J Neurosci. 8(6):1991–2002.

Freund TF, Katona I. 2007. Perisomatic inhibition. Neuron. 56(1):33–42.

Galarreta M, Hestrin S. 2002. Electrical and chemical synapses among parvalbumin fast-spiking GABAergic interneurons in adult mouse neocortex. Proc Natl Acad Sci U S A. 99(19):12438–12443.

Gibson JR, Beierlein M, Connors BW. 1999. Two networks of electrically coupled inhibitory neurons in neocortex. Nature. 402(6757):75–79.

Graber KD, Prince DA. 2006. Chronic partial cortical isolation. In: Models of seizures and epilepsy. In: Pitkanen A, Schwartzkroin P, Moshe S, editors. San Diego (CA): Elsevier Academic Press, p. 477–493.

Graber KD, Prince DA. 1999. Tetrodotoxin prevents posttraumatic epileptogenesis in rats. Ann Neurol. 46(2):234–242.

Hoffman SN, Salin PA, Prince DA. 1994. Chronic neocortical epileptogenesis in vitro. J Neurophysiol. 71(5):1762–1773.

Jacob TC, Moss SJ, Jurd R. 2008. GABA(A) receptor trafficking and its role in the dynamic modulation of neuronal inhibition. Nat Rev Neurosci. 9(5):331–343.

Jankowsky JL, Patterson PH. 2001. The role of cytokines and growth factors in seizures and their sequelae. Prog Neurobiol. 63(2):125–149.

Jefferys JG, Traub RD. 1998. 'Dormant' inhibitory neurons: do they exist and what is their functional impact? Epilepsy Res. 32:104–113.

Jin X, Huguenard JR, Prince DA. 2005. Impaired Cl^- extrusion in layer V pyramidal neurons of chronically injured epileptogenic neocortex. J Neurophysiol. 93(4):2117–2126.

Jin X, Prince DA, Huguenard JR. 2006. Enhanced excitatory synaptic connectivity in layer V pyramidal neurons of chronically injured epileptogenic neocortex in rats. J Neurosci. 26(18):4891–4900.
Jin X, Huguenard JR, Prince DA. 2007. Excitation and inhibition of neocortical fast-spiking interneurons in a model of posttraumatic epileptogenesis assessed with laser scanning photostimulation. Abstract of the annual conference of the Society for Neuroscience. 165:13.
Kawaguchi Y, Kubota Y. 1997. GABAergic cell subtypes and their synaptic connections in rat frontal cortex. Cereb Cortex. 7:476–486.
Kharazia VN, Jacobs KM, Prince DA. 2003. GluR1 and calbindin expression are altered in interneurons of neocortical microgyral malformations. Neurosci. 120:207–218.
Kobayashi. 2003. Buckmaster PS. 2003. Reduced inhibition of dentate granule cells in a model of temporal lobe epilepsy. J Neurosci. 23(6):2440–2452.
Kotti T, Riekkinen PJ Sr, Miettinen R. 1997. Characterization of target cells for aberrant mossy fiber collaterals in the dentate gyrus of epileptic rat. Exp Neurol. 146(2):323–330.
Kumar SS, Jin X, Buckmaster PS, Huguenard JR. 2007. Recurrent circuits in layer II of medial entorhinal cortex in a model of temporal lobe epilepsy. J Neurosci. 7;27(6):1239–1246.
Larsen DD, Callaway EM. 2006. Development of layer-specific axonal arborizations in mouse primary somatosensory cortex. J Comp Neurol. 494(3):398–414.
Li H, Prince DA. 2002. Synaptic activity in chronically injured, epileptogenic sensory-motor neocortex. J Neurophysiol. 88(1):2–12.
Ma YY, Prince DA. 2009. Decreased inhibition in chronically epileptogenic neocortex due to abnormalities in presynaptic terminals of fast-spiking interneurons. American Epilepsy Society Abstracts. 3.052.
Magloczky Z, Freund TF. 2005. Impaired and repaired inhibitory circuits in the epileptic human hippocampus. Trends Neurosci. 28:334–340.
Marchenko VG, Pasikova NV, Kositsyn NS. 2004. Intracortical synchronization of epileptic discharges at different stages of ultrastructural rearrangements in a completely neuronally isolated area of rat neocortex. Neurosci Behav Physiol. 34(4):307–313.
Marco P, DeFelipe J. 1997. Altered synaptic circuitry in the human temporal neocortex removed from epileptic patients. Exp Brain Res. 114(1):1–10.
Marco P, Sola RG, Pulido P, Alijarde MT, Sanchez A, Cajal SY, DeFelipe J. 1996. Inhibitory neurons in the human epileptogenic temporal neocortex—an immunocytochemical study. Brain. 119: 1327–1347.
Markram H, Toledo-Rodriguez M, Wang Y, Gupta A, Silberberg G, Wu C. 2004. Interneurons of the neocortical inhibitory system. Nat Rev Neurosci. 5(10):793–807.
Nabekura J, Ueno T, Okabe A, Furuta A, Iwaki T, Shimizu-Okabe C, Fukuda A, Akaike N. 2002. Reduction of KCC2 expression and GABAA receptor-mediated excitation after in vivo axonal injury. J Neurosci. 22(11):4412–4417.
Ogiwara I, Miyamoto H, Morita N, Atapour N, Mazaki E, Inoue I, Takeuchi T, Itohara S, Yanagawa Y, Obata K, et al. 2007. Na(v)1.1 localizes to axons of parvalbumin-positive inhibitory interneurons: a circuit basis for epileptic seizures in mice carrying an Scn1a gene mutation. J Neurosci. 27(22):5903–5914.
Pathak HR, Weissinger F, Terunuma M, Carlson GC, Hsu FC, Moss SJ, Coulter DA. 2007. Disrupted dentate granule cell chloride regulation enhances synaptic excitability during development of temporal lobe epilepsy. J Neurosci. 27(51):14012–14022.
Povysheva NV, Gonzalez-Burgos G, Zaitsev AV, Kröner S, Barrionuevo G, Lewis DA, Krimer LS. 2006. Properties of excitatory synaptic responses in fast-spiking interneurons and pyramidal cells from monkey and rat prefrontal cortex. Cereb Cortex. 16(4):541–552.
Prince DA, Parada I, Scalise K, Graber K, Jin X, Shen F. 2009. Epilepsy following cortical injury: cellular and molecular mechanisms as targets for potential prophylaxis. Epilepsia. 50(2 Suppl):30–40.
Ragozzino D, Palma E, Di Angelantonio S, Amici M, Mascia A, Arcella A, Giangaspero F, Cantore G, Di Gennaro G, Manfredi M, et al. 2005. Rundown of GABA type A receptors is a dysfunction associated with human drug-resistant mesial temporal lobe epilepsy. Proc Natl Acad Sci U S A. 102(42):15219–15223.
Ribak CE, Harris AB, Vaughn JE, Roberts E. 1979. Inhibitory, GABAergic nerve terminals decrease at sites of focal epilepsy. Science. 205(4402):211–214.
Rosen GD, Jacobs KM, Prince DA. 1998. Effects of neonatal freeze lesions on expression of parvalbumin in rat neocortex. Cereb Cortex. 8:753–761.
Rutecki PA, Lebeda FJ, Johnston D. 1987. 4-Aminopyridine produces epileptiform activity in hippocampus and enhances synaptic excitation and inhibition. J Neurophysiol. 57:1911–1924.
Salin PA, Prince DA. 1996. Electrophysiological mapping of GABAA receptor-mediated inhibition in adult rat somatosensory cortex. J Neurophysiol. 75(4):1589–1600.
Salin PA, Tseng GF, Hoffman SN, Parada I, Prince DA. 1995. Axonal sprouting in layer V pyramidal neurons of chronically injured cerebral cortex. J Neurosci. 15:8234–8245.
Scharfman HE, Sollas AL, Berger RE, Goodman JH. 2003. Electrophysiological evidence of monosynaptic excitatory transmission between granule cells after seizure-induced mossy fiber sprouting. J Neurophysiol. 90(4):2536–2547.
Schubert D, Kotter R, Luhmann HJ, Staiger JF. 2006. Morphology, electrophysiology and functional input connectivity of pyramidal neurons characterizes a genuine layer Va in the primary somatosensory cortex. Cereb Cortex. 16(2):223–236.
Schubert D, Staiger JF, Cho N, Kötter R, Zilles K, Luhmann HJ. 2001. Layer-specific intracolumnar and transcolumnar functional connectivity of layer V pyramidal cells in rat barrel cortex. J Neurosci. 21:3580–3592.
Shen F, Fu K, Li J, Parada I, Bacci A, Prince DA. Inhibitory connections of fast-spiking GABAergic interneurons are altered in chronically epileptogeneic rat neocortex. Epilepsia. 8(46 Suppl):124.
Sloviter RS. 1987. Decreased hippocampal inhibition and a selective loss of interneurons in experimental epilepsy. Science. 2. 235(4784): 73–76.
Sloviter RS, Zappone CA, Harvey BD, Frotscher M. 2006. Kainic acid-induced recurrent mossy fiber innervation of dentate gyrus inhibitory interneurons: possible anatomical substrate of granule cell hyper-inhibition in chronically epileptic rats. J Comp Neurol. 494(6):944–960.
Somogyi P, Tamas G, Lujan R, Buhl EH. 1998. Salient features of synaptic organization in the cerebral cortex. Brain Res Brain Res Rev. 26:113–135.
Spreafico R, Battaglia G, Arcelli P, Andermann F, Dubeau F, Palmini A, Olivier A, Villemure J, Tampieri D, Avanzini G, et al. 1998. Cortical dysplasia, an immunocytochemical study of three patients. Neurology. 50:27–36.
Stepanyants A, Tamás G, Chklovskii DB. 2004. Class-specific features of neuronal wiring. Neuron. 43(2):251–259.
Stevens B, Allen NJ, Vazquez LE, Howell GR, Christopherson KS, Nouri N, Micheva KD, Mehalow AK, Huberman AD, Stafford B, Sher A, Litke AM, Lambris JD, Smith SJ, John SW, Barres BA. 2007. The classical complement cascade mediates CNS synapse elimination. Cell. 14;131(6):1164–1178.
Sutula T. 2002. Seizure-induced axonal sprouting: assessing connections between injury, local circuits, and epileptogenesis. Epilepsy Curr. 2:86–91.
Sutula TP, Dudek FE. 2007. Unmasking recurrent excitation generated by mossy fiber sprouting in the epileptic dentate gyrus: an emergent property of a complex system. Prog Brain Res. 163:541–563.
Thomson AM. 1997. Activity-dependent properties of synaptic transmission at two classes of connections made by rat neocortical pyramidal axons in vitro. J Physiol. 502:131–147.
Thomson AM, Bannister AP. 2003. Interlaminar connections in the neocortex. Cereb Cortex. 13(1):5–14.

Trotter SA, Kapur J, Anzivino MJ, Lee KS. 2006. GABAergic synaptic inhibition is reduced before seizure onset in a genetic model of cortical malformation. J Neurosci. 26(42):10756–10767.

Uematsu M, Hirai Y, Karube F, Ebihara S, Kato M, Abe K, Obata K, Yoshida S, Hirabayashi M, Yanagawa Y, et al. 2008. Quantitative chemical composition of cortical GABAergic neurons revealed in transgenic venus-expressing rats. Cereb Cortex. 18:315–330.

Weiss JH, Koh J, Baimbridge KG, Choi DW. 1990. Cortical neurons containing somatostatin- or parvalbumin-like immunoreactivity are atypically vulnerable to excitotoxic injury in vitro. Neurology. 40(8):1288–1292.

Xiang Z, Huguenard JR, Prince DA. 2002. Synaptic inhibition of pyramidal cells evoked by different interneuronal subtypes in layer v of rat visual cortex. J Neurophysiol. 88(2):740–750.

Zhang W, Yamawaki R, Wen X, Uhl J, Diaz J, Prince DA, Buckmaster PS. 2009. Surviving hilar somatostatin interneurons enlarge, sprout axons, and form new synapses with granule cells in a mouse model of temporal lobe epilepsy. J Neurosci. 29:14247–14256.

Zhou FW, Chen HX, Roper SN. 2009. Balance of inhibitory and excitatory synaptic activity is altered in fast-spiking interneurons in experimental cortical dysplasia. J Neurophysiol. 102:2514–2525.

Zhu WJ, Roper SN, Roper SN. 2000. Reduced inhibition in an animal model of cortical dysplasia. J Neurosci. 20:8925–8931.